Generation of non-overlapping fiber architecture

Chapelle, Lucie; Lévesque, M. ; Brøndsted, Povl; Foldschack, M. R. ; Kusano, Yukihiro

Published in:
Proceedings of the 20th International Conference on Composite Materials

Publication date:
2015

Document Version
Publisher's PDF, also known as Version of record

GENERATION OF NON-OVERLAPPING FIBER ARCHITECTURE

L. Chapelle[1,2], M. Lévesque[3], P. Brøndsted[2], M. R. Foldschack[1], Y. Kusano[2]

[1]Group Development, ROCKWOOL International A/S,
Hovedgaden 584, DK-2640 Hedehusene, Denmark
E-mail: lucie.chapelle@rockwool.com, web page: http://rockwool.com
Email: mathilde.foldschack@rockwool.com, web page: http://rockwool.com

[2]Department of Wind Energy, Technical University of Denmark
P.O. Box 49, Frederiksborgvej 399, DK-4000 Roskilde, Denmark
Email: pobr@dtu.dk, web page: http://www.dtu.dk

[3] Laboratory for Multiscale Mechanics (LM2), CREPEC, Département of Mechanical Engineering,
École Polytechnique de Montréal, C.P. 6079, succ. Centre-ville, Montréal, QC, H3C3A7, Canada
Email: martin.levesque@polymtl.ca, web page: http://www.polymtl.ca/lm2

Keywords: Random periodic packing, Curved fibers, Fiber orientation

ABSTRACT

Numerical models generating actual fiber architecture by including parameters such as the fiber geometry and arrangement are a powerful tool to explore the relation between the fiber architecture and mechanical properties. The generation of virtual architectures of fibrous materials is the first step toward the computation of their physical properties. In this work, a realistic 3D model is developed to describe the architecture of a complex fiber structure. The domain of application of the model could include natural fibers composites, wood fibers materials, papers, mineral and steel wools and polymer networks. The model takes into account the complex geometry of the fiber arrangement in which a fiber can be modeled with a certain degree of bending while keeping a main fiber orientation. The model is built in two steps. First, fibers are generated as a chain of overlapping spheres or as a chain of overlapping sphero-cylinders. At the end of the first step, a system of overlapping fibers is obtained. In order to obtain a hard-core configuration where fibers cannot overlap other fibers, we use an iterative method called the force-biased algorithm. It applies virtual forces on each point of the fiber: a repulsion force to suppress the overlap between two fibers and a bending and stretching force to ensure that the fiber structure is kept unchanged. The model can be used as the geometrical basis for further finite-element modelling.

1 INTRODUCTION

The generation of a packing of objects in a space can either be designated as a soft-core or hard-core process. In a soft-core model, the overlap of the packed object is allowed which is not realistic from a physical point of view. However the simplicity of implementation of those processes has made it a quite popular tool for the microstructure generation of complex materials. One of the first soft-core processes generating a packing of fibers was introduced by Matheron [1]. It made use of dilated Poisson lines to create straight infinite cylinders [1]. Later, lines were generated by a Poisson process in [2–5] to model respectively the microstructure of a nonwoven material, the gas diffusion layer of proton exchange membrane fuel cells and the fiber structure of thermal and acoustic materials. Soft-core models were developed further to consider fibers with a more complex geometry. For example, to model curved fiber system, several soft-core processes include bending of the fibers through random walks whose direction are controlled by von Mises-Fischer distribution [6, 7]. Others have introduced bending of the fibers by interpolating points with B-splines [8, 9].
The random sequential adsorption (RSA) model is probably the most commonly used method to construct hard-core systems because its principle is relatively simple even though its implementation can be a bit tricky for objects with a complex geometry. The RSA scheme iteratively generates objects and tries to place them in such a way that they do not intersect. Initially created for the packing of

spheres, the process was then applied on cylinders by Feder [10]. Bezrukov and Stoyan proposed an algorithm for the generation of random packing of ellipsoids of revolution [11]. Contacts between ellipsoids are detected and a force biased algorithm is applied to translate and rotate the particles that overlap. Both approaches achieve relatively low volume fraction (10 – 15 % for isotropic orientation with a fiber aspect ratio of 10). Recently, Naddeo et al. used an RSA based microstructure generation method with fibers shaped as cylinders but very little details on the overlap detection was provided [12]. On the other hand, in [13], the implementation of the contact detection of two cylinders is given. The problem of the RSA based method is that for fibers with an isotropic orientation distribution and high aspect ratio, only low volume fractions can be achieved as a jamming limit is reached when no new positions can be found. Modifications of the RSA algorithm can be made so that when a fiber position is rejected because it overlaps another fiber with a certain distance, a translation of this distance is applied to the fiber. Using this algorithm, microstructures with volume fractions up to 38 and 29% and randomly oriented fibers with aspect ratios of 10 and 30, respectively, were generated [14].

Another type of model based on the deposition of straight fibers can achieve hard-core configurations [15]. In that model, fibers are deposited in an iterative manner from the top of the cell and whenever they enter in contact with another fiber, they stop their falls. This approach gives high fiber volume fraction, but the fiber orientation is limited to the plane. The deposition technique is widely used for paper-like materials where the assumption of an in-plane fiber orientation distribution is quite realistic [16–18]. The fiber bending model was also included in [19]. When an overlap is detected, fibers are bent to accommodate the intersection with other fibers. Straight fibers are modelled as convex prism with two dodecagon end-faces while several convex irregular polyhedral are used in case of curved fibers. Wang et al. modeled non-woven fiber-webs by a similar deposition algorithm where the orientation was limited to a plane [20].
Some other hard-core models took inspiration in molecular dynamics simulations. For example, Ghossein et al. used an event-driven molecular dynamics algorithm to generate spheres and ellipsoids with a very high aspect ratio (i.e.>10) in a hard-core packing configuration [21, 22]. Recently, Altendorf et al. presented a model combining some of the ideas discussed previously [23]. Firstly, bended fibers are modelled as ball chains by a random walk [24]. Secondly, similar to Wirjadi [6] and Karkkainen et al. [7] the orientation distribution can be controlled in spite of the bending. Thirdly, the force-biased approach is applied for sphere packing [25] and [11] and fourthly, the design of energies in molecular dynamics is used to define the forces [25]. It produces a random hard-core fiber model with a controllable bending and high volume fraction. The level of bending is controlled by two parameters in the multivariate von Mises Fisher distribution. As mentioned earlier, the fibers are represented as chains of spheres with defined centers and radii. The spheres are connected through random walk paths. This first step gives a soft-core system of bending fibers. To produce a hard-core configuration, a force biased approach is used. Two kinds of forces are applied to the sphere centers: repulsion and recover forces. The repulsion force prevents the overlap of fibers and the recover force maintains the sphere chain structure. Gaiselmann et al. also represented the fibers by a chain of spheres but generated the fibers midpoints with a Poisson point process and the fibers by random 3D polygonal tracks [26]. The overlap of the fibers was suppressed using a force-biased algorithm as well [25].

In the present work, a modified version of the algorithm from Altendorf et al. [23] is implemented. The modification includes the use of a chain of sphero-cylinders for the fiber model, the possibility of modeling the fiber bending using spline interpolation and the introduction of more realistic forces for the transformation into a non-overlapping fiber network.

2 GENERATION OF A SOFT-CORE FIBERS NETWORK

2.1 Fiber model

2.1.1 Chain of spheres

The first model studied in this work is the one adopted from [23, 27] where a fiber is modelled as a chain of overlapping spheres. The coordinates of the first sphere center of the chain are generated according to a uniform law in the intervals $[0 - x_{max}]$, $[0 - y_{max}]$ and $[0 - z_{max}]$ where x_{max}, y_{max} and z_{max} are the length of the sides of the observation cell chosen for the generation. The coordinates of a point $i \in \mathbb{N}\backslash\{0\}$ representing the center of a sphere belonging to the fiber are generated iteratively from the coordinates of their previous neighbor $\mathbf{x_{i-1}}$:

$$\mathbf{x_i} = \mathbf{x_{i-1}} + \boldsymbol{\mu_i} \cdot \frac{r_i}{2} \tag{1}$$

r_i and $\boldsymbol{\mu_i}$ are respectively the fiber radius and the direction of the fiber at the point i. A realization of a fiber is shown in the figure below (Fig. 1).

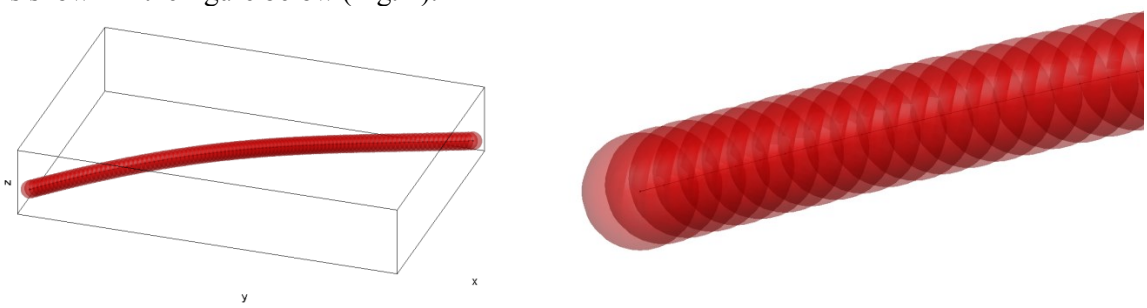

Figure 1: Fiber modelled as a chain of spheres

2.1.2 Chain of sphero-cylinder

A new discretization is proposed here where the fiber is modelled as a chain of overlapping sphero-cylinders. The generation process is similar to the one proposed in section 2.1.1. The only difference is the length of the step between two points. The first spherical part of the sphero-cylinder overlaps with the spherical part of the previous sphero-cylinder. If μ_i designates the direction, l_i the height of the cylinder part and x_{i-1} the position of its previous neighbour, then the position of the point i is:

$$\mathbf{x_i} = \mathbf{x_{i-1}} + \boldsymbol{\mu_i} \cdot l_i \tag{2}$$

The geometry of the sphero-cylinder and a fiber modelled by a walk of points obtained using the sphero-cylinder model are represented in the figure below (Fig. 2).

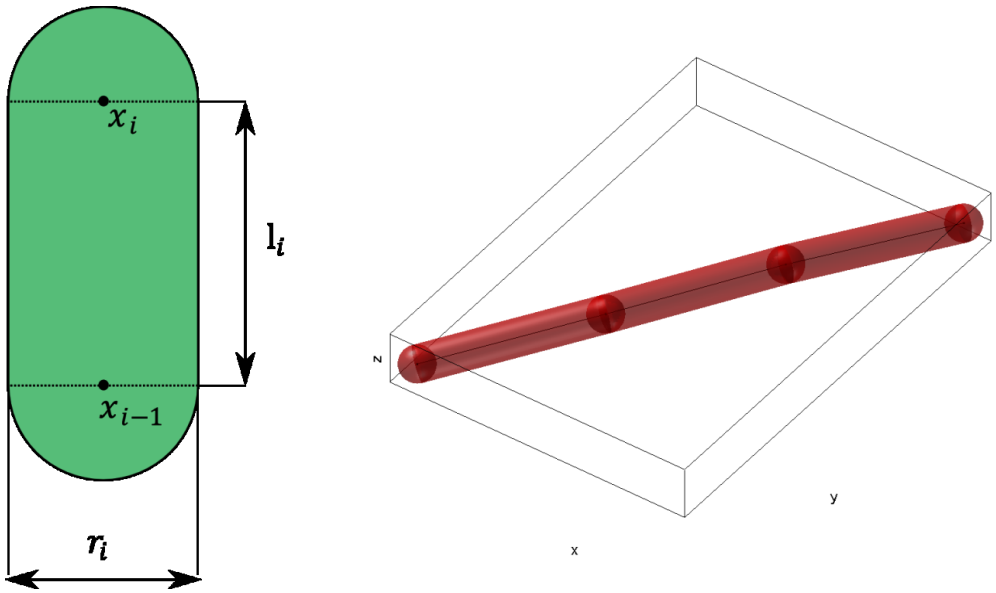

Figure 2: Fiber modelled as a chain of sphero-cylinders

2.2 Models for the fiber orientation

2.2.1 Main fiber orientation

The distribution proposed in [2] was chosen to define the orientation of the fibers. The density associated to this distribution is a function $p_\beta(\theta, \varphi)$ of elevation $\theta \in [0, \pi)$ and azimuth $\varphi \in [0, \pi)$:

$$p_\beta(\theta, \varphi) = \frac{1}{4\pi} \frac{\beta \sin\theta}{(1 + (\beta^2 - 1)\cos\theta)^{3/2}} \tag{3}$$

$\beta \in \mathbb{R}+\backslash\{0\}$ is the anisotropy parameter. We can notice that the distribution is independent from φ. The angles definition and a plot of the probability density function for two values of β is given in Fig. 3.

The case $\beta = 1$ describes an isotropic fiber system and results in the uniform distribution on the sphere. For increasing β the fibers tend to be more and more parallel to the xy-plane. For $\beta \to 0$, the distribution concentrates around the z-axis.

To sample directions selected from the distribution, the inverse cumulative distribution $G(\theta)$ is needed. Indeed, if u is a uniform variable on [0,1], then $G^{-1}(u)$ follows the distribution given by G. The cumulative distribution $G(\theta)$ is given by:

$$G(\theta) = \frac{1}{2} - \frac{\beta}{2\sqrt{\cos^{-2}\theta + (\beta^2 - 1)}} \tag{4}$$

And the inverse of $G(\theta)$ is:

$$G^{-1}(x) = \cos^{-1}\left(\frac{x}{\sqrt{x^2 - \beta x^2 + \beta^2}}\right) \tag{5}$$

The following procedure is applied:

1) x_1 and x_2 are sampled from a uniform distribution in (0,1)
2) Find θ such that $x_1 = G(\theta)$: $\theta = G^{-1}(x_1)$
3) Find φ such that $x_2 = F(\varphi)$: $\varphi = 2\pi x_2$

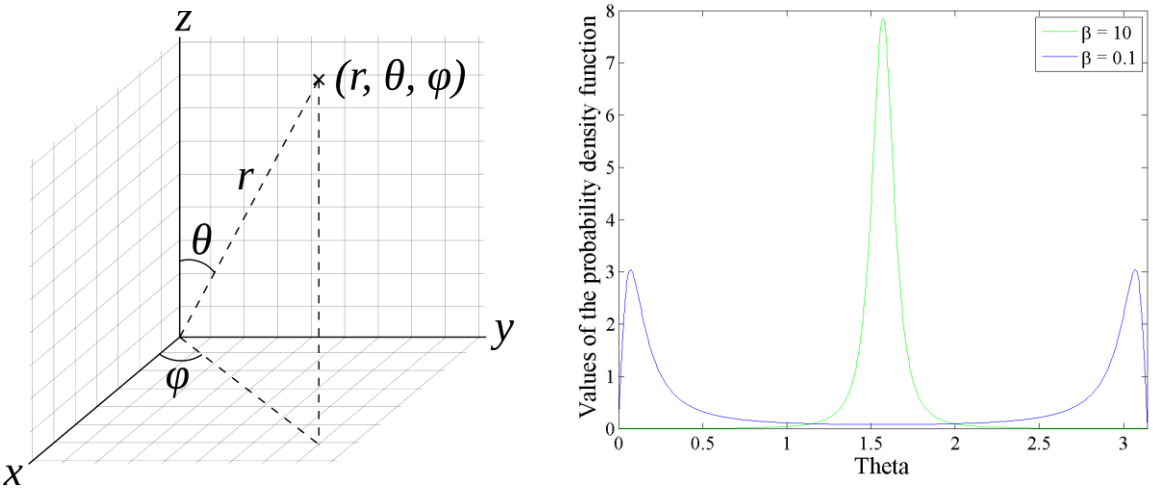

Figure 3: Angle definition and probability density function for the β distribution with $\beta = 10$ and $\beta = 0.1$

Figure 4 shows different realization of an overlapping fiber network with different values of β.

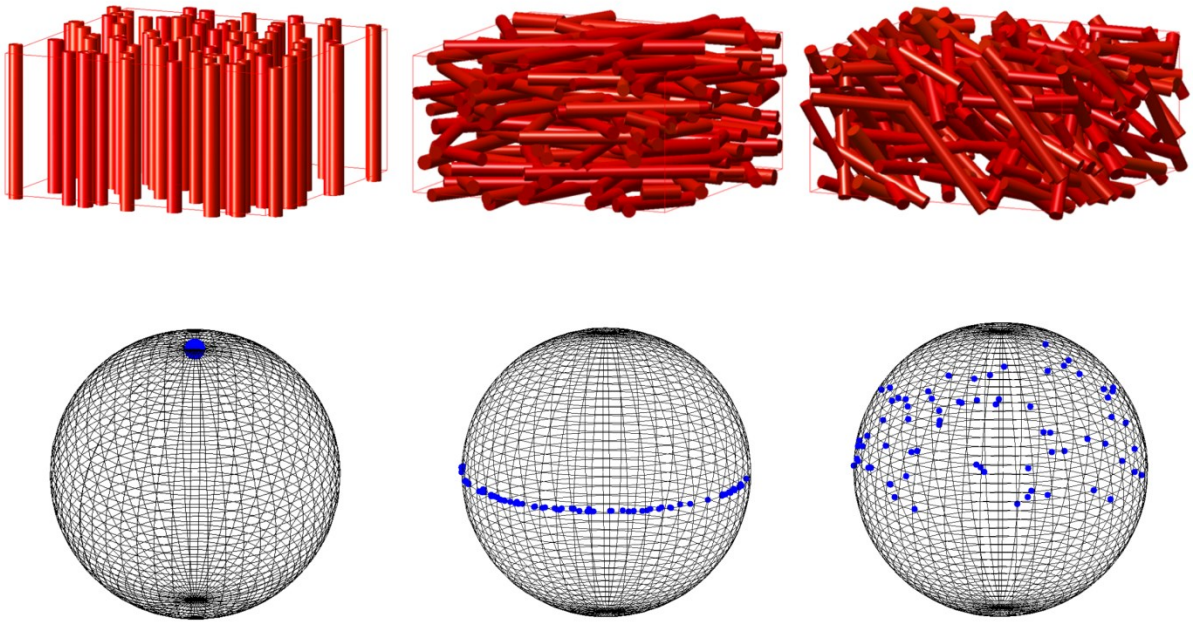

Figure 4: Top: Realization with $\beta = 0$ (left), $\beta = 100$ (middle) and $\beta = 1$ (right). Bottom: corresponding directions on the unit sphere

2.2.2 Fiber bending using von-Mises Fischer distribution

The von-Mises Fischer (vMF) distribution is a well-known distribution used to describe the orientation of objects with a preferred direction and a reliability parameter. The probability density element of a vMF distribution for a vector u with a preferred direction vector μ and a reliability parameter κ is:

$$f(u|\mu,\kappa) = \frac{\kappa}{2\pi(e^{\kappa} - e^{-\kappa})} e^{\kappa \mu^T u} \tag{6}$$

We present in table 1 the algorithm for sampling a vector from a vMF distribution. Details of the implementation can be found in [28, 29].

Kärkkainen et al. and later Altendorf and Jeulin have extended the univariate von Mises-Fischer distribution to a multivariate one in order to make use of two preferred directions and two reliability parameters [7, 23]. One of the preferred directions is the main fiber orientation while the other is set to be the direction of the previous element of the fiber.

The probability density function of a bivariate von Mises-Fischer distribution for a sampled direction $\mathbf{u}$ with preferred directions $\boldsymbol{\mu_1}$ and $\boldsymbol{\mu_2}$ and corresponding reliability parameters , κ_1 and κ_2 is:

$$f(u|\boldsymbol{\mu_1},\kappa_1,\boldsymbol{\mu_2},\kappa_2) = \frac{|\kappa_1\boldsymbol{\mu_1} + \kappa_2\boldsymbol{\mu_2}|}{2\pi(e^{|\kappa_1\boldsymbol{\mu_1}+\kappa_2\boldsymbol{\mu_2}|} - e^{-|\kappa_1\boldsymbol{\mu_1}+\kappa_2\boldsymbol{\mu_2}|})} e^{(\kappa_1\boldsymbol{\mu_1}^T\mathbf{u}+\kappa_2\boldsymbol{\mu_2}^T\mathbf{u})^T\mathbf{u}} \tag{7}$$

To generate random directions following a bivariate von Mises-Fischer distribution, we use the same algorithm as presented before as the bivariate function can be written as a classical von Mises-Fischer distribution by setting:

$$\kappa = |\kappa_1 \boldsymbol{\mu_1} + \kappa_2 \boldsymbol{\mu_2}| \text{ and } \boldsymbol{\mu} = \frac{\kappa_1 \boldsymbol{\mu_1} + \kappa_2 \boldsymbol{\mu_2}}{\kappa} \tag{8}$$

Table 1: Sampling a vector from a vMF distribution

Algorithm 1

A. Define a vector $\mathbf{w_k}$ with mean direction $\boldsymbol{\mu} = (0,0,1)^T$ distributed according to a vMF distribution
B. $\mathbf{w_k} = (\sqrt{1 - W^2}\mathbf{V}, W)^T$ where $\mathbf{V}$ and W are independent random variables, $\mathbf{V} \in \mathbb{R}^2$ is a uniformly distributed vector on the unit circle, and $W \in [-1; 1]$ follow the density: $f(v|\kappa) = \frac{\kappa}{(e^{\kappa} - e^{-\kappa})} e^{\kappa v}$
    1. Compute the cumulative function of f: $F(x) = \frac{\kappa}{(e^{\kappa} - e^{-\kappa})} \left(\frac{1}{\kappa} e^{\kappa x} - \frac{1}{\kappa} e^{-\kappa}\right)$
    2. Compute the inverse of F: $F^{-1}(y) = \frac{1}{\kappa} \log\left(e^{-\kappa} + \kappa \frac{e^{\kappa} - e^{-\kappa}}{\kappa} y\right)$
    3. Draw a scalar y from a uniform distribution in the interval (0,1)
    4. Compute W: $F^{-1}(y) = W$
    5. Draw a variable $\mathbf{V}$ from a uniform distribution on the unit circle
    6. Compute $\mathbf{w_k} = (\sqrt{1 - W^2}\mathbf{V}, W)^T$
C. Apply a rotation matrix to generate a vector with a mean direction other than $(0,0,1)^T$

2.2.3 Bending introduced by splines

In this approach, a line is generated in 3D using the orientation distribution defined in 2.2.1 and curvature points are added around this line by adding a deviation parameter to points belonging to the line.

$$\mathbf{p_{2i}} = \mathbf{p_{1i}} + \Delta\mathbf{s} = \begin{pmatrix} x_{1i} \\ y_{1i} \\ z_{1i} \end{pmatrix} + \begin{pmatrix} \Delta s_x \\ \Delta s_y \\ \Delta s_z \end{pmatrix} \tag{9}$$

The points are then used as control points to generate a cubic spline. The degree of curvature and tortuosity of a fiber can be controlled by adjusting the number of points that deviates from the line and the deviation parameter, $\Delta\mathbf{s}$.

2.3 Generation of a system with overlapping fibers

A system with overlapping fibers is created using either the chain of spheres or chain of sphero-cylinders approach. The bending and orientation of the chain is described by the distribution described in section 2.2. The algorithm for the generation of a system of overlapping fibers is given in table 2.

Table 2: Generation of a system of overlapping fibers

Algorithm 2:

A. Ask for inputs for the fiber main orientation (β), the fibre bending ($\kappa_1, \boldsymbol{\mu_1}, \kappa_2, \boldsymbol{\mu_2}$ or $\Delta\mathbf{s}$), the fibre aspect ratio, the fiber volume fraction (V_f) and the size of the cell
B. Initialize variables (current volume V, array containing the future fibre data points)
C. **WHILE** $\|V - V_f\| \leq$ small number
    1. **WHILE** $\|$desired aspect ratio $-$ current aspect ratio$\| \leq$ small number
        i. $\mathbf{x_i} = \mathbf{x_{i-1}} + \boldsymbol{\mu_i} \cdot l_i$
    2. **END WHILE**
    3. **IF** points exits through a face
        i. Create a periodic images
        ii. Delete element completely outside of the cell
    4. **END IF**
D. **END WHILE**

At the end of this step, a periodic system with overlapping fibers is obtained with controlled orientation, bending and aspect ratio of the fibers.

3 GENERATION OF A HARD-CORE FIBRE NETWORK

To transform the overlapping system of fibers into a hard-core one, we use the force-biased algorithm first introduced by Moscinski et al. for the packing of hard spheres [25]. Virtual forces are applied on overlapping spheres until the overlap is completely prevented. Later, Altendorf and Jeulin extended the force-biased algorithm to fiber structure and added two additional forces that ensure that the fiber stretching and bending is constrained as well [23]. In this work, the expressions for the forces are expressed as a function of the material properties. The forces are applied by small increment until the total energy of the system reaches a minimum threshold level.

3.1 Repulsion forces

The force needed to repulse two objects overlapping is inspired from the Hertz contact between two hard surfaces where the overlap is treated as the deformation.

$$F_{repulsion} = K_r \left(\frac{r_1 r_2}{r_1 + r_2}\right) \delta^{3/2} \tag{10}$$

The algorithm for the implementation of the repulsion force is presented in table 3.

For a fast implementation of the repulsion force, the search of candidate points that are susceptible to overlap is optimized by using a near neighbor list [30]. The cell containing the fibers is divided into smaller sub-cells. The neighbors of a point are searched in the cell where the point belongs as well as the adjacent cells.

Table 3: Repulsion force for two spheres or sphero-cylinders that overlaps

Algorithm 3
A. Compute distance between the two centers or minimal distance between the axis of the sphero-cylinders $d_{i,j}$
B. Calculate the overlap: $\delta = \max(0, r_i + r_j - d_{i,j})$
C. Calculate the force and potential
1. **IF** $d_{i,j} = 0$
ii. Create a unit random direction vector $\mathbf{u} = 2 \cdot \mathrm{rand}(3,1) - 1$
i. $\mathbf{F_{repulsion}} = K_r \left(\frac{r_1 r_2}{r_1 + r_2}\right) \delta^{3/2} \mathbf{u}$
2. **ELSE**
ii. $\mathbf{F_{repulsion}} = K_r \left(\frac{r_1 r_2}{r_1 + r_2}\right) \delta^{\frac{3}{2}} \cdot \left(\frac{x_j - x_i}{\|x_j - x_i\|}\right)$
3. **END IF**

3.2 Bending and tension forces

To ensure that the fiber keeps its structure while being under the action of the repulsion forces, two forces are introduced that constraint the relative motion of the elements of the fibers. The first one is limiting the stretching of the fiber axis. It acts like a spring with a constant K_S and is a function of the elongation:

$$F_{stretching} = \frac{K_S}{l_0}\left(\frac{l_i - l_0}{l_0}\right) \tag{10}$$

where l_0 is the intial distance between two elements (spheres or sphero-cylinders) and l_i is the current

distance after the application of forces. The forces are applied at the centers of the spherical parts of the sphero-cylinder or at the centers of the spheres depending on the elements chosen for the discretization of the fiber.

Under tensile load, the strain and the stress can be expressed as:

$$\varepsilon = \frac{l_0 - l_i}{l_0} \text{ and } \sigma = \frac{F}{S} = \frac{K_S}{l_0 \pi r^2}\left(\frac{l_i - l_0}{l_0}\right) \tag{11}$$

By analogy with Hooke´s law, we identify the spring constant K_S as:

$$K_S = E_F l_0 \pi r^2 \tag{12}$$

The bending of the three consecutives elements of a fiber is also constrained by another force acting like a torsional spring with a constant K_B:

$$F_{bending} = K_B(\theta_i - \theta_0) \tag{13}$$

where θ_0 the intial angles between three consectutives points and θ_i the current angle. A simple system with three consecitive points (i, j, k) that can be either the centers of overlapping spheres or the centers of the spherical parts of the sphero-cylinders is displayed in the figure below (Fig. 5).

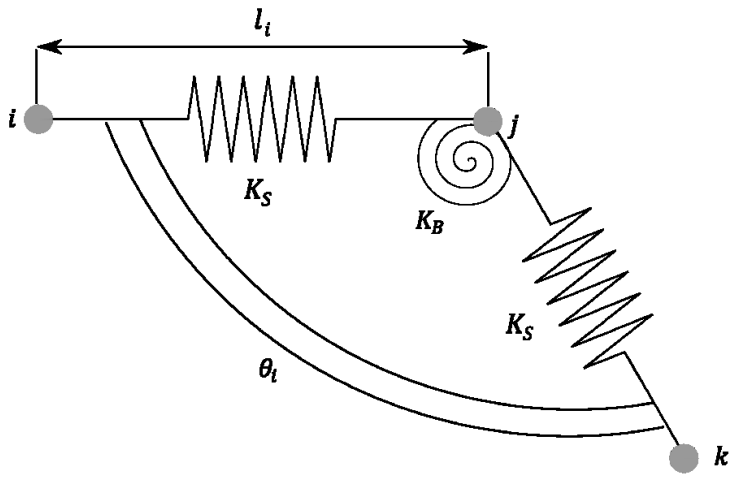

Figure 5: Representation of the system considered for the application of the forces

We also seek to express the constant K_B as a material parameter. Consider a fiber discretized in N elements (spheres or sphero-cylinders) clamped in one end and loaded with a force F in the other end. Assuming that the work in tension/compression is negligible, we show that the potential energy E is:

$$E = \sum_{i=1}^{N-2}\left(\frac{1}{2}K_B(\theta_i - \pi)^2\right) - F\delta \tag{14}$$

where δ is the deflection (Fig. 6).

We assume small strains and expressed the deflection as the sum of the displacement as a function of the current angles θ_i:

$$\frac{x_i}{l_0} = \sin(\pi - \theta_i) \approx \pi - \theta_i \Rightarrow \frac{\delta}{l_0} = \sum_{i=1}^{N-2}(N - i - 1)(\pi - \theta_i) \tag{15}$$

The beam is in equilibrium when the energy reaches a minimal value. Thus we derive the energy and solve θ_i for the equation $\frac{\partial E}{\partial \theta_i} = 0$

$$\frac{\partial E}{\partial \theta_i} = K_B(\theta_i - \pi) + Fl_0(N - i - 1) = 0 \Leftrightarrow \pi - \theta_i = \frac{Fl_0}{K_B}(N - i - 1) \tag{16}$$

Replacing $(\theta_0 - \theta_i)$ in equ. (13) and using the expression of the sum of squares:

$$\frac{\delta}{l_0} = \sum_{i=1}^{N-2} \frac{Fl_0}{K_B} \cdot (N - i - 1)\,(N - i - 1) = \frac{Fl_0}{6K_B}(N - 2)(N - 1)(2N - 3) \tag{17}$$

Normalizing with the diameter D of the fibre:

$$\frac{\delta}{D} = \frac{F}{3}\left(\frac{L}{D}\right)^3 \cdot \left(\frac{D^2}{K_B l_0}\right)\left(1 - \frac{l_0}{L}\right)\left(1 - \frac{l_0}{2L}\right) \tag{18}$$

By analogy with the beam theory, we obtain an expression for the bending constant depending on material parameters:

$$\frac{\delta}{D} = \frac{FD^2}{3E_f I}\left(\frac{L}{D}\right)^3 = \frac{F}{3}\left(\frac{L}{D}\right)^3 \cdot \left(\frac{D^2}{K_B l_0}\right)\left(1 - \frac{l_0}{L}\right)\left(1 - \frac{l_0}{2L}\right) \Leftrightarrow K_B = \frac{E_f I}{l_0}\left(1 - \frac{l_0}{L}\right)\left(1 - \frac{l_0}{2L}\right) \tag{19}$$

And if the length of the elements is negligible compared to the length of the fiber, we obtain:

$$K_B \approx \frac{E_f I}{l_0} \tag{20}$$

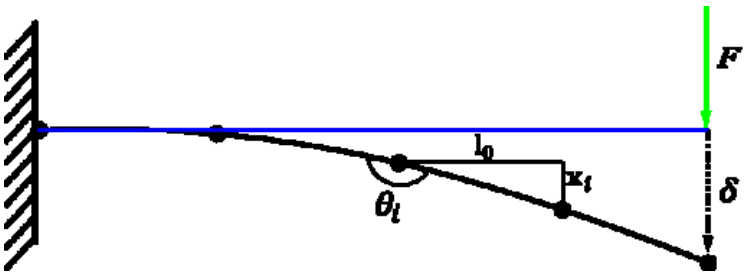

Figure 6: bending of a discretized fiber

3.3 Examples of hard-core fibers network

Figure 7 shows the realization of two hard-core fibers networks. Their main characteristics are defined in table 4. We control the fiber radius distribution by drawing the values from a lognormal law. By adjusting the value of the scale parameter σ of the lognormal law, the spread of the distribution can be tuned. Based on the radius and the aspect ratio we calculate the total length of the fiber and the number of discretization points for the fiber model.

Table 4: Parameter for fibers network generation

	Fiber model	Fiber volume fraction	Aspect ratio	Main fiber orientation (β)	Bending
A	Sphero-cylinders	10 %	50	50	mvMF ($\kappa_1 = 5$ and $\kappa_2 = 500$)
B	Spheres	10 %	50	50	mvMF ($\kappa_1 = 5$ and $\kappa_2 = 500$)
C	Sphero-cylinders	10 %	50	50	splines
D	Spheres	10 %	50	50	splines

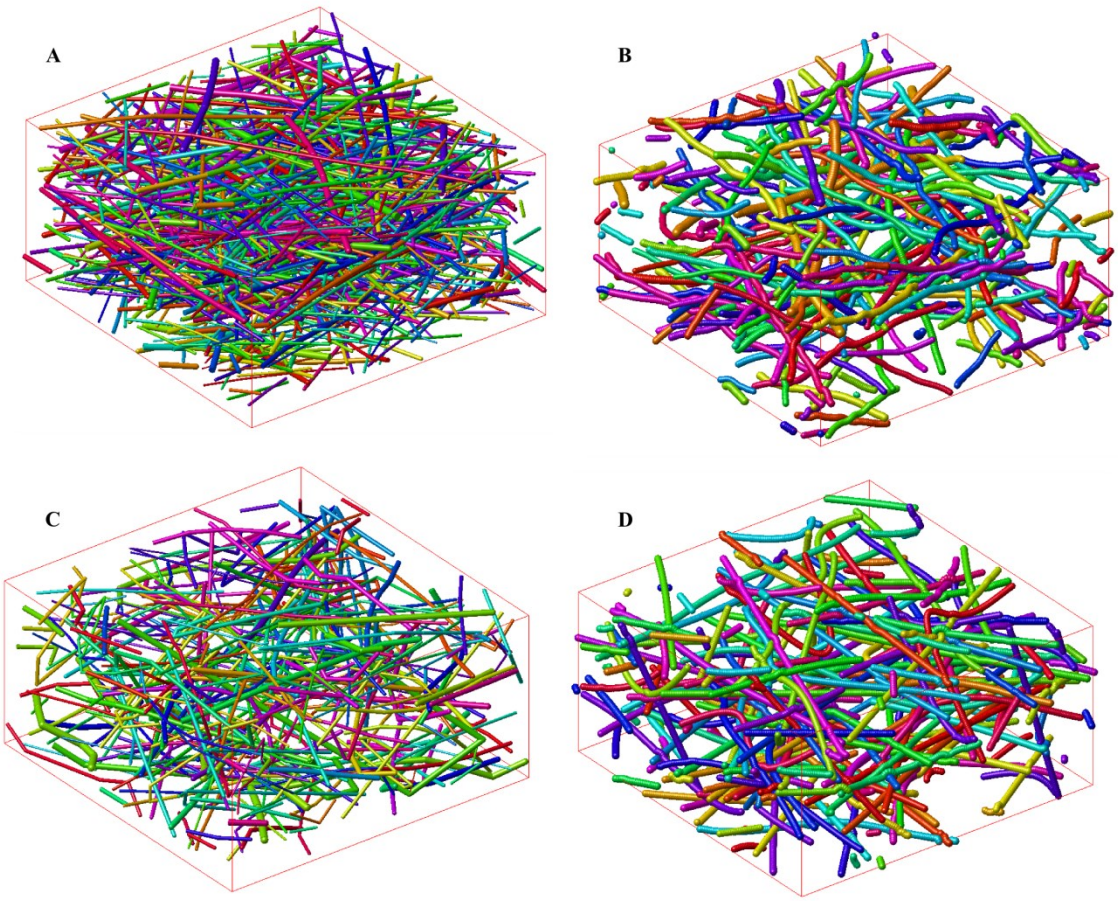

Figure 7: Realization of hard-core fibers systems

4 DISCUSSION & CONCLUSION

We present here a modification of the algorithm originally proposed by Altendorf and Jeulin for the generation of a system of hard-core fibers [23]. In the modified algorithm, the fiber is modeled as a chain of sphero-cylinders rather than a chain of spheres. This implementation reduces the computational effort for the transformation of the overlapping system into a non-overlapping one as fewer points are considered when applying the forces. The bending of the fibers can be controlled using either a multivariate von Mises-Fischer distribution or a cubic b-spline interpolation. A near-neighbor list is built to determine which points are susceptible to overlap. This increases significantly the speed of the algorithm. The forces applied during the transformation of the system into a non-overlapping one are expressed as a function of material parameters and geometry.

REFERENCES

1. Matheron, G.: Random sets and integral geometry. , New York (1975).
2. Schladitz, Katja, Peters Stefanie, Reinel-Bitzer Doris, Wiegmann, Andreas, Ohser, J.: Design of acoustic trim based on geometric modeling and flow simulation for non-woven. Comput. Mater. Sci. 38, 56 – 66 (2006).
3. Thiedmann, R., Fleischer, F., Hartnig, C., Lehnert, W., Schmidt, V.: Stochastic 3D Modeling of the GDL Structure in PEMFCs Based on Thin Section Detection. J. Electrochem. Soc. 155, B391 (2008).
4. Peyrega, C., Jeulin, D., Delisée, C., Lux, J.: 3D Morphological modelling of a random fibrous network. Image Anal. Stereol. 28, 129–141 (2009).
5. Dirrenberger, J., Forest, S., Jeulin, D.: Towards gigantic RVE sizes for 3D stochastic fibrous networks. Int. J. Solids Struct. 51, 359–376 (2014).
6. Wirjadi, O.: Models and Algorithms for Image-Based Analysis of Microstructures, (2009).
7. Kärkkäinen, S., Miettinen, A., Turpeinen, T., Nyblom, J., Pötschke, P., Timonen, J.: a Stochastic Shape and Orientation Model for Fibres With an Application To Carbon Nanotubes. Image Anal. Stereol. 31, 17–26 (2012).
8. Faessel, M., Delisée, C., Bos, F., Castéra, P.: 3D Modelling of random cellulosic fibrous networks based on X-ray tomography and image analysis. Compos. Sci. Technol. 65, 1931–1940 (2005).
9. Durville, D.: Numerical simulation of entangled materials mechanical properties. J. Mater. Sci. 40, 5941–5948 (2005).
10. Feder, J.: Random sequential adsorption. J. Theor. Biol. 87, 237–254 (1980).
11. Bezrukov, A., Stoyan, D.: Simulation and Statistical Analysis of Random Packings of Ellipsoids. Part. Part. Syst. Charact. 23, 388–398 (2006).
12. Naddeo, F., Cappetti, N., Naddeo, A.: Automatic versatile parametric procedure for a complete FEM structural analysis of composites having cylinder-shaped reinforcing fibres. Comput. Mater. Sci. 81, 239–245 (2014).
13. Pan, Y.: Stiffness and Progressive Damage Analysis on Random Chopped Fiber Composite Using FEM, (2010).
14. Moussady, H.: A new definition of the representative volument element in numerical homogenization problems and its application to the performance evaluation of analytical homogenization models, (2013).
15. Provatas, N., Haataja, M., Asikainen, J., Majaniemi, S., Alava, M., Ala-Nissila, T.: Fiber deposition models in two and three spatial dimensions. Colloids Surfaces A Physicochem. Eng. Asp. 165, 209–229 (2000).
16. Ekman, A., Miettinen, A., Turpeinen, T., Backfolk, K., Timonen, J.: The number of contacts in random fibre networks. Nord. Pulp Pap. Res. J. - Pap. Phys. 27, 270–276 (2012).
17. Kulachenko, A., Uesaka, T.: Direct simulations of fiber network deformation and failure. Mech. Mater. 51, 1–14 (2012).
18. Curto, Joana M R, Eduardo, L.T.: The fibre properties influence on a three dimensional paper model. XXI TECNICELPA Conference and Exhibition/VI CIADICYP. , Lisbon, Portugal (2010).
19. Pan, Y., Iorga, L., Pelegri, A. a.: Numerical generation of a random chopped fiber composite RVE and its elastic properties. Compos. Sci. Technol. 68, 2792–2798 (2008).
20. Wang, Q., Maze, B., Tafreshi, H.V., Pourdeyhimi, B.: Simulating through-plane permeability of fibrous materials with different fiber lengths. Model. Simul. Mater. Sci. Eng. 15, 855–868 (2007).
21. Ghossein, E., Lévesque, M.: Random generation of periodic hard ellipsoids based on molecular dynamics: A computationally-efficient algorithm. J. Comput. Phys. 253, 471–490 (2013).
22. Ghossein, E., Lévesque, M.: A fully automated numerical tool for a comprehensive validation of homogenization models and its application to spherical particles reinforced composites. Int. J. Solids Struct. 49, 1387–1398 (2012).

23. Altendorf, H., Jeulin, D.: Random-walk-based stochastic modeling of three-dimensional fiber systems. Phys. Rev. E. 83, 041804 (2011).
24. Rodney, D., Fivel, M., Dendievel, R.: Discrete Modeling of the Mechanics of Entangled Materials. Phys. Rev. Lett. 95, 108004 (2005).
25. Moscinski, J., Bargiel Monika, Rycerz; Katarzyna, Jacobs Patrick: The Force-Biased Algorithm for the Irregular Close Packing of Equal Hard Spheres. Mol. Simul. 3, (1989).
26. Gaiselmann, G., Froning, D., Tötzke, C., Quick, C., Manke, I., Lehnert, W., Schmidt, V.: Stochastic 3D modeling of non-woven materials with wet-proofing agent. Int. J. Hydrogen Energy. 38, 8448–8460 (2013).
27. Joung, C.G., Phan-Thien, N., Fan, X.J.: Direct simulation of flexible fibers. J. Nonnewton. Fluid Mech. 99, 1–36 (2001).
28. Jung, S.: "Generating von Mises Fisher distribution on the unit sphere(s2). relation. 1993–1994 (2009).
29. Ulrich, G.: Computer Generation of distributions on the m-sphere. J. R. Stat. Soc. 33, 158–163 (1984).
30. Mattson, W., Rice, B.M.: Near-neighbor calculations using a modified cell-linked list method. Comput. Phys. Commun. 119, 135–148 (1999).